

# The first data from the Orion laser: measurements of the spectrum of hot dense aluminium

D J Hoarty<sup>1</sup>, P Allan<sup>1</sup>, S F James<sup>1</sup>, C R D Brown<sup>1</sup>, L M R Hobbs<sup>1</sup>, M P Hill<sup>1</sup>, J W O Harris<sup>1</sup>, J Morton<sup>1</sup>, M G Brookes<sup>1</sup>, R Shepherd<sup>2</sup>, J Dunn<sup>2</sup>, H Chen<sup>2</sup>, E Von Marley<sup>2</sup>, P Beiersdorfer<sup>2</sup>, H K Chung<sup>3</sup>, R W Lee<sup>4</sup>, G Brown<sup>3</sup>, J Emig<sup>3</sup>.

1 Directorate of Research and Applied Science, AWE plc, Reading, RG7 4PR, UK

2 Lawrence Livermore National Laboratory, 7000 East Avenue, Livermore, CA94550, USA

3 Nuclear Data Nuclear Data Section, Division of Physical and Chemical Sciences, International Atomic Energy Agency, P. O. Box 100, A-1400, Vienna, Austria

4 Institute for Material Dynamics at Extreme Conditions, University of California, Berkeley, USA.

David.Hoarty@awe.co.uk

**Abstract.** The newly commissioned Orion laser system has been used to study dense plasmas created by a combination of short pulse laser heating and compression by laser driven shocks. Thus the plasma density was systematically varied between 1 and 10g/cc by using aluminium samples buried in plastic foils or diamond sheets. The aluminium was heated to electron temperatures between 500eV and 700eV allowing the plasma conditions to be diagnosed by K-shell emission spectroscopy. The K-shell spectra show the effect of the ionization potential depression as a function of density via the delocalization of n=3 levels and disappearance of n=3 transitions in He-like and H-like aluminium. The data are compared to simulated spectra, which account for the change in the ionization potential by the commonly used Stewart and Pyatt prescription; a simple ion sphere model and an alternative due to Ecker and Kröll suggested by recent X-ray free-electron laser experiments. The experimental data are in reasonable agreement with the model of Stewart and Pyatt, but are in better agreement with a simple ion sphere model. The data indicate that the Ecker and Kröll model overestimates substantially the ionization potential depression in this regime.

## 1. Introduction/Background

A new laser facility called Orion [1] has been commissioned at AWE in the UK which combines long pulse, nanosecond timescale, and short pulse, picosecond timescale, laser beam technologies. As part of the facility commissioning a series of experiments was carried out where samples were heated to electron temperatures over the range 500eV to 700eV and the plasma density was varied systematically over an order of magnitude between 1-10g/cc. The samples were aluminium layers buried in either plastic foils or diamond sheets. At such high densities the electrostatic field of neighbouring ions and electrons acts on the outer levels of the ions lowering the ionization energy of the dense plasma ions relative to the isolated ion case. The experiments described here show the effect of ionization potential depression (IPD) on the emitted spectra as a function of density by the disappearance of line emission



from the  $n=3$  levels in He-like and H-like aluminium ions. There has been a renewal of interest in IPD due the findings of recent X-ray free electron laser experiments (XFEL) at the Linac Coherent Light Source (LCLS) facility [2].

The Orion experiments extend work carried out on the HELEN laser between 2006 and 2009. Experiments on HELEN showed that a thin buried layer in plastic could be heated to high temperature in excess of 500eV and in some cases up to 1keV [3]. The conditions were diagnosed by modelling the details of the aluminium K-shell emission in the 1.5-3.0 keV energy range from aluminium ionized to He-like and H-like configurations by modelling the spectra with the atomic kinetics code FLY [4] and its successor FLYCHK [5]. Measurements were made using both a 1.5 ps temporal resolution streak camera coupled to a focussing crystal spectrometer [6] and time-integrating X-ray crystal spectrometers recording onto X-ray film or BAS-TR Fuji image plates [7]. Examples of the spectrum of aluminium recorded on HELEN are given Ref [3]. The first experiments on Orion were carried out to investigate the heating of buried layer targets using the infrared beam. These experiments confirmed the findings of the HELEN experiments that coupling of laser energy to heating the bulk solid target is poor in the presence of significant pre-pulse [3]. The effectiveness of the second harmonic conversion in improving solid target heating was demonstrated in a series of shots using targets with an overcoat of plastic between the laser and the buried layer, which was varied between  $5\mu\text{m}$  up to  $35\mu\text{m}$  on a shot by shot basis. The rear plastic coating was  $2\mu\text{m}$  as in the previously reported HELEN experiments [3]. The data showed heating to temperatures above 500eV up to a depth of  $25\mu\text{m}$  and a sharp fall off in peak electron temperature between 25 and  $35\mu\text{m}$  [3].

## 2. Compressed plastic experiments on Orion

In the planar compression and short pulse heating of the buried layer targets the ablation pressure from the long-pulse laser drives a shock wave through the foil and into the buried layer [3]. The material between the buried layer and the laser is sufficiently thick that the laser does not ablate through to the buried layer before the end of the laser pulse. In order to heat the compressed foil the short-pulse beam is initiated when the transiting shock is between the buried layer position and the rear face of the foil. Combined long-pulse compression and short-pulse heating was applied to plastic targets where the ablative layer irradiated with the long-pulse beams was a  $12\mu\text{m}$  thick coating of plastic and on the other side of the buried aluminium tracer the coating was  $10\mu\text{m}$  of plastic. The shock driven through the  $12\mu\text{m}$  ablator by long-pulse laser ablation compressed the layer and the plastic tampers. Before shock breakout at the rear of the target the short-pulse beam heated the target to high temperature. The experiment used Orion long-pulse beams each with a pulse length of 0.5ns FWHM at  $0.35\mu\text{m}$  wavelength and energy of 180-200J. The short-pulse beam was converted to second harmonic operation as described above. The long pulses were shaped with an approximately 100ps rising edge. The emissivity of the aluminium sample was obtained in absolute units ( $\text{J/keV/sr/cm}^2/\text{s}$ ) as described in Ref [3] along with further details of the experiment. Preheating of the aluminium layer caused it to expand into the surrounding plastic ahead of the arrival of the shock. However, experiments using two of the Orion beams were able to demonstrate compression above twice solid in aluminium and heating to a temperature in excess of 500eV. The spectral ranges of the instruments were set to record the K-shell emission from aluminium ionized to He-like and H-like configurations. The time-integrating spectrometers recorded the  $n=1-2$  and  $n=1-3$  transitions; the time-resolved data covered the  $n=1-3$  only, due to restrictions on the spectral dispersion and streak camera slit length with the streak camera. This overlap in the spectrum allowed comparison of ratios from time-integrated and time-resolved data as in the HELEN experiments. The time-integrated data are shown in Fig. 1 along with a fit using the FLY code. In Fig 1 the prediction was scaled by 1.17 to achieve the agreement shown in the figure. This was within the experimental error of 30% for the measured emissivity.

The line-ratios of the  $n=1-3$  transitions in the 1.8-2.2keV energy range are used to infer the temperature and the overall width of the line shape is used to establish the density. This is accurate despite the disagreement at line centre where the code predicts a dip in the profile that is much more pronounced than in the experimental data. The peak electron temperature inferred from the data is

550eV and the density 6g/cc. The data from the 1.5ps resolution streak camera are shown in the inset plot in Fig. 1 along with a curve generated using the FLY code [4]. The best fit to the time-resolved data is at a slightly higher temperature of 600eV and a density of 6g/cc compared to the time-integrated case. This slightly higher peak temperature in the time-resolved data is typical of the comparison between time-integrated and time-resolved data where the best fit to the time-integrated data tended to be 50-80eV lower than the time-resolved data on the same shot. Sensitivity studies have shown that the spectra are more sensitive to temperature than density [3]. The density fit at 7g/cc is a poorer fit to the  $\text{He}_\beta$  line width and the 5g/cc is narrower than the experimental width of  $\text{Ly}_\beta$ . Fits using FLYCHK [5] and the ALICE [8] atomic physics and line-shape codes infer the same conditions. Similar experiments in the same campaign that used different samples of aluminium buried in diamond sheets have demonstrated even higher temperatures and densities. These experiments are described in the next section

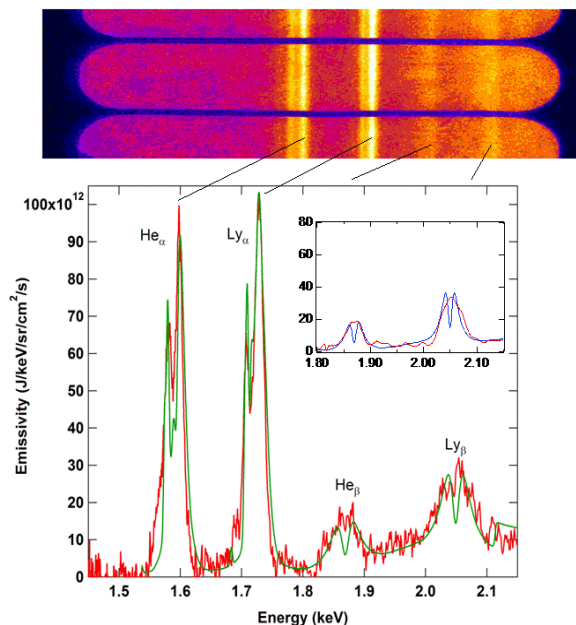


Fig 1: Time-integrated data from long-pulse compression and short-pulse heating of aluminium buried in plastic foil. The spectrometer data is shown and a lineout of the spectrum recorded. Also shown is the best fit to the data using the FLY atomic kinetics and line-shape code. The fit indicates a peak electron temperature of 550eV and a peak density of 6g/cc which meets the criteria for the milestone. The predicted emissivity has been scaled by a factor 1.17.

### 3. Experiments with aluminium samples in diamond

The maximum density achievable in the buried layer is determined by pressure equilibration with the compressed tamper material when the material in the layer expands into the tamper after heating and ionization [3]. The targets with high-density tampers used a combination of diamond, which was grown as a wafer, and diamond-like carbon, which was coated onto the target. To get the two diamond layers to bond a thin coating of silicon carbide was applied between them. The diamond targets were designed to prevent expansion of the aluminium buried sample into the surrounding tamper due to preheat by the long-pulse beams during the transit of the shock wave through the ablator layer. The 10 $\mu\text{m}$  diamond sheet was used as the target ablator for the long-pulse beam and the short-pulse beam irradiated the 4 $\mu\text{m}$  diamond-like carbon side to heat the compressed target through to the buried layer. First tests of the diamond targets were to examine the response to short-pulse heating alone. Comparison of this data to FLY calculations allowed the temperature and density conditions in the

aluminium to be inferred. The peak electron temperature was  $750\pm 50\text{eV}$  and the material density was inferred to be  $3.5\pm 0.5\text{g/cc}$ . Experiments using a long-pulse beam of Orion to drive a shock through the diamond had the laser wavelength, pulse shape, focal spot and energy identical to that of the beams used in the aluminium in plastic foil experiments described above. The relative delay between the long-pulse and short-pulse beam was varied to step through the time history of the shock compression and short pulse heating of the target. The results are shown in Fig. 2 for the spectral range covered by the streak camera, which is the  $n=3$  transitions in He-like and H-like aluminium ions. Figure 2 shows the effect of shock compression on the line emission from the aluminium dot buried in diamond. The long-pulse beam is initiated before the short-pulse beam and drives a shock wave which takes 280ps to arrive at the aluminium layer. This shock transit time was confirmed by examination of the background silicon emission on selected targets from the batch of diamond targets as described below.

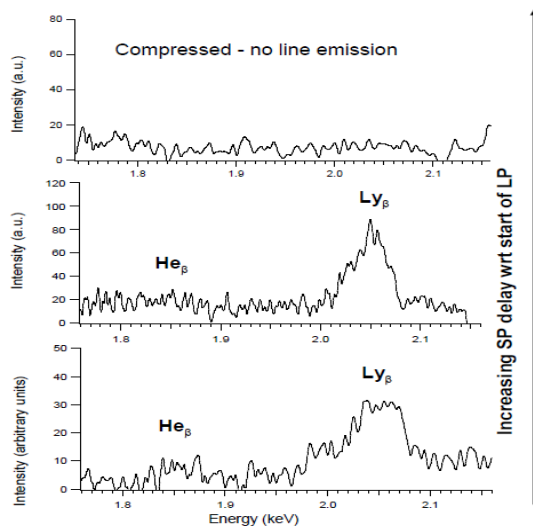


Fig 2: The graphs are streaked spectra taken at different long pulse-short pulse delay. Once compressed the  $n=1-3$  transitions from the aluminium disappear.

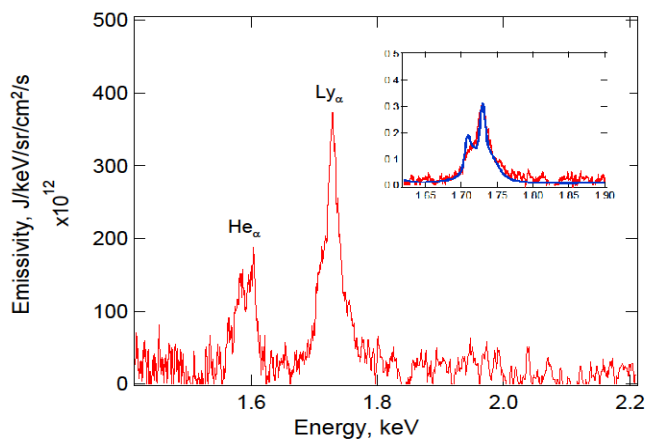


Fig 3: Time-integrated data from compressed aluminium in diamond. The curve is a lineout through the spectrum after image processing to remove background noise and allow for image plate and filter responses. The inset curve shows a fit to the experimentally measured  $\text{Ly}_\alpha$  line (red curve) of the prediction from the atomic physics and line-shape model FLY (blue curve) indicates a density of  $9\pm 1\text{g/cc}$ . A peak electron temperature from the He/Ly line ratio was inferred to be  $700\pm 50\text{eV}$ .

The bottom curve of Fig. 2 was taken from streak data where the long-pulse shock had not yet arrived at the aluminium and shows clear emission from  $\text{He}_\beta$  and  $\text{Ly}_\beta$  lines. The middle curve was also

taken prior to the shock arrival and shows the same lines clearly. However, in the top curve where the long pulse was initiated 300ps early the shock has compressed the sample but not yet broken out from the rear surface of the diamond sheet. The streak data at this time do not show the line emission seen at earlier times. This disappearance of the  $n=1-3$  lines in the spectrum is due the delocalization of the  $n=3$  level in the He-like and H-like aluminium ions so that the levels blend into the free-bound continuum. In the absence of the  $n=1-3$  transitions in the streak-camera data the  $n=1-2$  transitions from He-like and H-like ions in the time-integrated data from compressed aluminium in diamond, shown in Fig. 3, were used to infer the sample conditions. Note that, as in the time-resolved data, the time-integrated data show no signature of the  $n=1-3$  transitions from the compressed aluminium. The inset curve in Fig. 3 shows the lineout through the time-integrated data for  $Ly_\alpha$  compared to a predicted line-shape using the FLY model. The line-shape predicted by FLY is the best fit to the time-integrated data in the  $Ly_\alpha$  line at  $9\pm 1\text{g/cc}$  and  $700\pm 50\text{eV}$ . The temperature was obtained from the ratio of He-like to H-like emission. However, it should be noted that the FLY code predicts that the  $n=1-3$  transitions are still clearly in evidence at  $9\text{g/cc}$  and  $700\text{eV}$  and are not delocalized as indicated in the data. Also, the satellite emission on the low energy side of the line, which is due to doubly-excited states of He-like ions, is clearly over-estimated in the simulation. Further evidence of the conditions is available from the shock transit times and the radiation-hydrodynamics simulations.

It was possible to measure the shock transit time in the diamond targets because of a flaw in some of them where the silicon wafer that the diamond sheet was grown on was not completely etched away. This left a residue of silicon on the face irradiated by the long-pulse beam within the long-pulse spot. On these targets there was a silicon emission signal marking the leading edge of the long pulse beam. The accuracy of the Orion timing system was confirmed by changing the inter-beam delay in 10ps increments and measuring the change in the measured delay with the streak camera using the diamond targets with a silicon residue. By establishing the shock transit time accurately the predictions of the NYM radiation hydrodynamics calculations [9] could be benchmarked with respect to the measured shock transit time. It was found that the irradiance used in the NYM code had to be reduced by 20% from the measured value in order to match the measured shock transit time. The calculated temperatures and densities from the NYM simulations, adjusted to reproduce the observed shock transit time predict values close to the conditions of  $9\pm 1\text{g/cc}$  and  $700\pm 50\text{eV}$  inferred from the time-integrated spectral measurements [3]. This confirms the aluminium in compressed diamond conditions inferred from the spectral measurements.

#### 4. Interpretation of the aluminium spectra

Traces of the aluminium spectra measured with the streak camera and crystal spectrometer in the range 1.8-2.2keV are shown in Fig. 4. The measurements at the various densities sampled experimentally show the conditions at which the  $n=3$  levels delocalize. Shown alongside the experimental data are predictions of the FLYCHK code using both the Stewart and Pyatt (SP) [10] and Ecker and Kröll (EK) [11] models of ionization potential depression (IPD), with the same prescription for SP and EK models used here as in Ref. [2]. The curves of both experiment and simulation are in arbitrary units and have been scaled in intensity for clarity. The experimental curves from bottom to top were fit at the following conditions of the total aluminium material density and peak electron temperature:  $1.2\pm 0.4\text{g/cc}$ ,  $550\text{eV}$ ;  $2.5\pm 0.3\text{g/cc}$ ,  $650\text{eV}$ ;  $4\pm 0.5\text{g/cc}$ ,  $700\text{eV}$ ;  $5.5\pm 0.5\text{g/cc}$ ,  $550\text{eV}$ ;  $9\pm 1\text{g/cc}$ ,  $700\text{eV}$ . The simulations use the measured density, but the temperature in all cases is  $700\text{eV}$ . The data show that  $n=3$  transitions are clearly observed up to densities of at least  $6\text{g/cc}$ , indicating that the IPD shift has not delocalized the  $n=3$  levels at this density. The spectral data and radiation-hydrodynamics simulations suggest that at a density between 8 and  $10\text{g/cc}$  the  $n=3$  levels are delocalized and that the  $n=1-3$  line transitions disappear from the spectrum [12]. The simulations using the SP prescription for IPD are in reasonable agreement with experiment but suggest that delocalization of the  $n=3$  levels, from bound states to the continuum, would occur at a slightly higher density ( $11.6\text{g/cc}$ ) than indicated by experiments. This curve is the top curve of the SP plots in Fig. 4. In contrast the simulations with

the EK model for IPD predict delocalization of  $n=3$  at much lower density due to the larger predicted shift in the bound-free edge due to ionization potential depression.

In summary, aluminium spectra have been measured at high temperature and density using samples buried in plastic foils and diamond sheet. The absolute emissivity is within 20% of predicted values and a systematic study of the aluminium spectrum varying the sample density, by a combination of short-pulse heating and long-pulse compression, has shown the conditions at which the  $n=3$  levels in He-like and H-like lines delocalize and the transitions merge into the continuum. The data show disagreement with the predicted conditions at which delocalization of  $n=3$  levels occurs in simulations of a time-dependent atomic kinetics model FLYCHK using a model of ionization potential depression due to Ecker and Kröll suggested by recent XFEL experiments [2]. The data indicate that at the range of the conditions sampled in these experiments the EK model overestimates the IPD shift significantly. The experimental data are in reasonable agreement with spectra predicted by FLYCHK using the SP model of IPD.

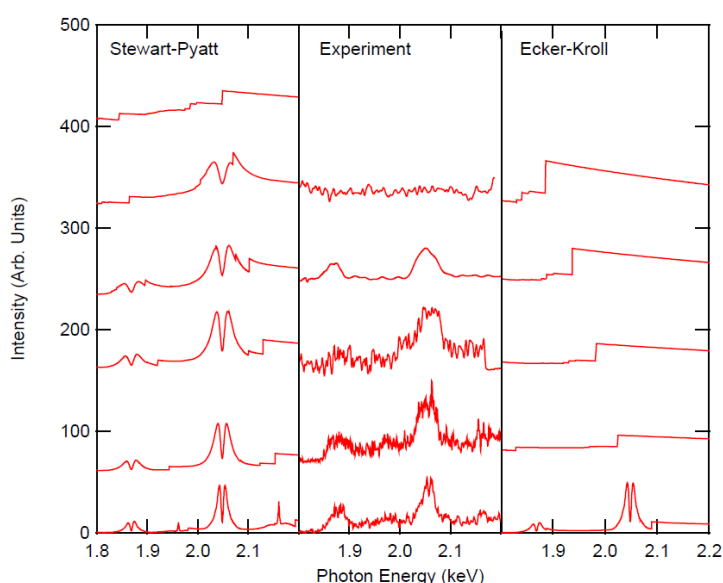


Fig 4: A compilation of the experimental data at different densities compared to FLYCHK predictions using Stewart and Pyatt and Ecker and Kröll treatments of ionization potential depression. The density of the curves from bottom to top is 1.2, 2.5, 4, 5.5 and 9g/cc. The SP plot has an additional curve at 11.6g/cc.

## References

- [1] N W Hopps et al, Proc. Of SPIE Vol 7916, 79160c DOI:10.1117/12.874252 (2011)
- [2] O Ciricosta et al, Phys. Rev. Lett. **109**, 065002 (2012)
- [3] D J Hoarty et al, High Energy Density Physics **9**, 661 (2013)
- [4] R W Lee and J T Larsen, J. Quant. Spectrosc. Radiat. Trans. **56**, 535 (1996)
- [5] H K Chung et al, High Energy Density Phys., **1**, 3 (2005)
- [6] C R D Brown et al, Phys. Rev. Letts. **106**, 185003 (2011)
- [7] N Izumi et al, Rev. Sci. Instrum. **77**, 10E325 (2006)
- [8] E Hill, private communication
- [9] P D Roberts et al., J. Phys. D **13**, 1957 (1980)
- [10] J C Stewart and K d Pyatt Jr. Astrophys. J. **144**, 1203 (1966)
- [11] G Ecker and W Kröll, Phys. Fluids **6**, 62 (1963)
- [12] D J Hoarty et al, Phys. Rev. Letts. **110**, 2656003 (2013)